Korean J. Chem. Eng., 33(5), 1692-1697 (2016)
DOI: 10.1007/s11814-015-0290-9

pISSN: 0256-1115
eISSN: 1975-7220

Densities and surface tensions of binary mixtures of biodiesel, diesel, and *n*-butanol

Hongya Yue† and Zhigang Liu

Key Laboratory of Thermo-Fluid Science and Engineering, Ministry of Education,
Xi'an Jiaotong University, Shaanxi Province 710049, P. R. China
(*Received 5 August 2015 • accepted 18 December 2015*)

Abstract−Density and surface tension have been measured for mixtures of biodiesel+*n*-butanol, biodiesel+diesel, and diesel+*n*-butanol over the entire concentration range at 283.15 K and 293.15 K and atmospheric pressure, with the combined expanded uncertainties of 1.32 kg·m^{-3} and 1%, receptively. Densities were determined by a single-sinker densimeter; surface tensions were measured using the surface laser light scattering method. The experimental data showed that densities and surface tensions decreased as temperature increased. The excess surface tensions and excess densities were all negative, and further fitted to the Redlich-Kister equation.

Keywords: Surface Tension, Surface Laser Light Scattering Method, Biodiesel, Diesel, *n*-Butanol

INTRODUCTION

Fuel shortages and environmental pollution are serious problems worldwide. Considerable attention has been focused on renewable oxygenate fuels, with particular reference to the biodiesel and alcohols [1-3]. Biodiesel fuel and *n*-butanol are non-fossil fuels that can be regarded as renewable energy because of reproducibility. For biodiesel-diesel fuel blends, researchers found that, compared with the diesel fuel, it could reduce CO and HC notably with slight increase of NO_x emission [4]. With adding of *n*-butanol as oxygenic additive, the combustion of diesel and biodiesel fuel can be improved dramatically. With this additive, CO and particulate matters (PM) can be reduced without increasing NO_x [5].

Density of fuel blends will directly affect the cetane number and heating value [6]. On the other hand, the change of density will influence the composition features of fuels, ignition quality, engine output power, and the concentration of exhaust-gas owning to the mass of fuel injected [7]. Surface tension is another key fuel property owning to its influence on fuel sprays and atomization processes. With small surface tension, the fuel drops will break up more easily, which will cause smaller Sauter Mean Diameter of spray and enhanced evaporation [8].

Due to its importance, researchers could present the results of combustion characteristics and exhaust emissions more easily when the densities and surface tensions of the fuel blends are known. However, reliable surface tension data are scarce now. We measured densities and surface tensions of blends of n-butanol+biodiesel, n-butanol+diesel, and biodiesel+diesel at 283.15-293.15 K and atmospheric pressure, which will provide the basic thermal properties to the related research.

†To whom correspondence should be addressed.
E-mail: yuehongya@stu.xjtu.edu.cn

EXPERIMENTAL SECTION

1. Materials

Biodiesel fuel was offered by Xi'an Blue Sky Biological Engineering Co. Ltd.; the commercial 0# diesel fuel was supplied by China Petroleum and Chemical Corporation; the properties of biodiesel and diesel fuels are shown in Tables 1 and 2, respectively. The samples of *n*-butanol were provided by Aladdin Industrial Corporation. The mass purity of *n*-butanol was better than 99.5%. All chemicals were used as received without further purification. The mixtures used were prepared by mass using an electronic balance (FA2204) with an accuracy ±0.1 mg, and the mass uncertainty was estimated to be less than 0.006.

2. Measurements

To maintain different temperatures, a thermostat bath with the temperature range of 233 to 363 K and the accuracy of ±0.01 K was used in this experiment, and the temperature was measured with a digital multimeter (Keithley 2010) and a Pt100 (±0.02 K) thermometer.

Densities of the samples were measured by hydrostatic method. A metal sinker was used to measure the buoyancy forces. The combined expanded uncertainty was estimated to be lower than 1.32 kg·m^{-3}. Surface tension of the binary mixtures was measured by using the surface laser light scattering method [9,10]. From the microscopic level, there exist thermally generated waves on the liquid surface, which were typically with small amplitude (~1 nm) and characteristic wavelength (~100 μm). Because each capillary wave acts optically as a diffraction grating, irradiated laser lights on the surface will be scattered, and the scattered light will be around the main reflection beam. As a result of Doppler effect, the scattered light is shifted in frequency, as shown in Fig. 1. The character of the scattered light is governed by the thermo properties of the liquid; thus thermo properties can be obtained through proper analysis of the scattered light.

Table 1. The relative contents of fatty acid methyl ester of biodiesel[a]

Components	Molecular formula	Molecular weight	Mass fraction%
Methyl tetradecanoate	$C_{15}H_{30}O_2$	242	2.56
Pentadecanoic acid	$C_{17}H_{34}O_2$	270	23.12
Octadecadienoic acid	$C_{19}H_{34}O_2$	294	31.22
Octadecenoic acid	$C_{19}H_{36}O_2$	296	20.41
Tetracontane	$C_{40}H_{82}$	562	4.32
Acetic acid	$C_{12}H_{24}O_2$	200	4.10
Dotriacontane	$C_{32}H_{66}$	450	5.16
Methyl stearate	$C_{19}H_{38}O_2$	298	2.35
15-Isobutyl-(13.alpha.H)-isocopalane	$C_{24}H_{44}$	332	4.15
Squalene	$C_{30}H_{50}$	410	2.61
Saponification value	Acid value	Water %	Iodine value
186 mg	3.16	0.012	99.2

[a]The relative content of fatty acid methyl ester of biodiesel was determined by using a chromatographic instrument (Agilent HP6890GC/5973MS)

Table 2. Properties of 0# commercial diesel fuel

Cetane number	T50	T90	T95	Viscosity mm^2/s 293.15 K	Sulfer
≥45	≤573	≤628	≤638	3.0	≤0.2%

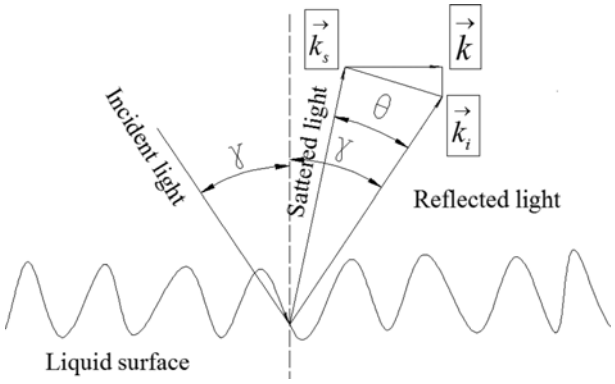

Fig. 1. The principle of surface laser light scattering.

Here $\vec{k}_i$ is the incident light wave number; γ is the incidence angle; $\vec{k}_s$ is the scattering light wave number; $\vec{k}$ is the liquid surface wave number; θ is the scattering angle. Compared with the liquid surface wave number, the incident light wave number is very large. We can approximately get: $|\vec{k}_i|=|\vec{k}_s|$. From the laws of geometrical optics [11]:

$$|\vec{k}|=|\sin\gamma-\sin(\gamma+\theta)|\vec{k}_i| \quad (1)$$

If the incidence angle γ=0:

$$|\vec{k}|=\sin(\theta)|\vec{k}_i| \quad (2)$$

where $|\vec{k}_i|=2\pi/\lambda_i$, λ_i is the wavelength of incident light. We can calculate the wave number of the capillary wave using the wavelength of the incident light and the scattering angle.

The motion of the thermally excited capillary waves was controlled by the thermophysical properties, especially surface tension and viscosity. From hydrodynamics [12]:

$$\sigma=\frac{\rho\omega_0^2}{k^3} \quad (3)$$

Here σ is the surface tension, ρ is the liquid density, $\omega_0=2\pi f$ is the angular frequency of the capillary waves, f is the frequency, and k is the wave number.

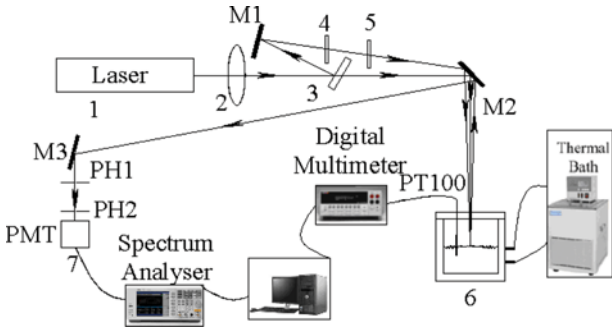

Fig. 2. Schematic diagram of SLLS experimental apparatus.

1. Laser
2. Convex lens (f=2,000 mm)
3. Beam split
4-5. Neutral density filter

M1-M3. Optically flat reflector
PH1-PH2. Pinhole
PMT. Photomultiplier tube

The experimental system is shown in Fig. 2, in which a 30 mW YAG laser beam was directed to convex lens to restrain beam extension; then the beam was led to a beam splitter and was separated into two beams [13]. By adjusting the mirrors M1, M2, the two beams intersect at the surface; then the scattered light of the incident light, which is perpendicular to the liquid surface, compound with the reference light, through PH1 and PH2 (pinhole), was detected by a PMT. Finally, the signals were fitted by the Lorentzian profile with peak angular frequency ω_0 using the least square method. To suppress the noise interference of light, a black cylinder, with 1m long and 50 mm in diameter, was placed in front of the photomultiplier tube. The samples and optical apparatus were installed on an optical desk to reduce external vibration.

3. Assessment of Uncertainties

The combined standard uncertainties of temperature can be given by [14]

$$u_c = \sqrt{\sum (u_i)^2} \quad (4)$$

where u_i is the uncertainty of each influencing factor which are platinum resistance thermometer, data collection and temperature stability, respectively.

The mass fraction w is calculated by

$$w = \frac{m_1}{m_1 + m_2} \quad (5)$$

where m_1 and m_2 are the mass of first and second component. The combined standard uncertainty of mass fraction is given by

$$u_c = \sqrt{\left(\frac{\partial w}{\partial m_1}\right)^2 u_{m_1}^2 + \left(\frac{\partial w}{\partial m_2}\right)^2 u_{m_2}^2 + u_{m_p}^2} \quad (6)$$

where u_{m_1}, and u_{m_2} are the uncertainties of m_1 and m_2. m_p is the uncertainty caused by chemical purity. The combined standard uncertainties of temperature, and mass fraction in this work are estimated to be less than 0.02 K, and 0.006, respectively.

The uncertainties of the densities are listed in Table 3. Inaddition, the uncertainties of surface tensions are associated with uncertainties of the measured quantities in Eq. (3), which were used to determine the surface tension. From literature [15], it can be expressed as:

$$\frac{\Delta\sigma}{\sigma}(k=2) \approx 2\sqrt{\left(\frac{\Delta\rho}{\rho}\right)^2 + 2\left(\frac{\Delta\omega}{\omega}\right)^2 + 3\left(\frac{\Delta k}{k}\right)^2} \quad (7)$$

where $\Delta\sigma/\sigma$ is the uncertainty of surface tension; $\Delta\rho/\rho$ is the uncertainty of density; $\Delta\omega/\omega$ is the uncertainty of angular frequency; $\Delta k/k$ is the unceratinty of wave number. The combined expanded uncertainties are 1% with a 0.95 level of confidence.

RESULTS AND DISCUSSION

The experimental densities and surface tensions of this work and related literature values of pure *n*-butanol at 283.15 K and 293.15 K are presented in Table 4. From Table 4, the relative deviations of densities and surface tension for pure *n*-butanol [16], compared with the literature values, were 0.23% and 0.59% at 283.15 K, 0.14% and 0.73% at 293.15 K, respectively, which indicated that the experimental results in this paper agree well with the literature values.

The combined expanded uncertainty of density is 1.32 kg·m^{-3}; the combined expanded uncertainty of density is 1%.

Densities, surface tensions, excess densities and surface tensions of the mixtures of biodiesel+1-butanol, biodiesel+diesel, and diesel +*n*-butanol detected at atmospheric pressure are given in Table 5. It can be seen that densities and surface tensions of these binary mixtures decreased as temperature increased. The excess thermodynamic properties were calculated by the following equations [20,21]:

$$\sigma^E = \sigma - x\sigma_1 - (1-x)\sigma_2 \quad (8)$$

$$\rho^E = \rho - x\rho_1 - (1-x)\rho_2 \quad (9)$$

Here, σ^E and ρ^E represent excess surface tension and excess density, respectively. σ and ρ represent surface tension and density. Subscripts 1 and 2 represent component 1 and component 2, respectively; x represents the mass fraction of component 1. The results of excess surface tensions and densities are listed in Table 5 and further fitted to Redlich-Kister type polynomial equation [22]:

$$\sigma^E = x(1-x)\sum_{i=0}^{k} A_i (2x-1)^i \quad (10)$$

$$\rho^E = x(1-x)\sum_{i=0}^{k} A_i (2x-1)^i \quad (11)$$

The combined expanded uncertainty of density is 1.32 kg·m^{-3}; the combined expanded uncertainty of density is 1%.

Here, A_i are the coefficients of the equation. The fitting curves of the surface tensions and densities were plotted in Figs. 2 and 3. In addition, the results of A_i are listed in Table 6 along with the standard deviation Y_{SD} which can be expressed [23]:

$$Y_{SD} = \left[\frac{\sum_{i=1}^{n}(Y_{exp} - Y_{calc})^2}{n-p}\right]^{1/2}, \quad (12)$$

Here, n is the number of data points, p is the number of the coefficients. The Y_{exp} and Y_{calc} represent the experiment and calculated value, respectively.

Figs. 3 and 4 illustrate the dependence of excess surface tension σ^E and excess densities ρ^E on concentration for biodiesel+*n*-butanol, biodiesel+diesel, diesel+*n*-butanol at 283.15 K and 293.15 K; the solid lines represent results calculated using Eqs. (6) and (7), respectively. For excess surface tensions, from Table 5 and Fig. 3, the values of σ^E are all negative over the whole range of compositions, displayng the minimum at x≈0.3, 0.5, 0.3 for x biodiesel+

Table 3. Experimental uncertainty of density

	Factor of uncertainty	Uncertainty
Density	Repeated trials	0.31 kg·m^{-3}
	The accuracy of measuring instrument	0.58 kg·m^{-3}
	Combined standard uncertainty	0.66 kg·m^{-3}
	The combined expanded uncertainty	1.32 kg·m^{-3}

Table 4. Densities, ρ, and surface tension, σ, of pure compounds at 283.15 K and 293.15 K and comparison with literature data

T/K	Compound	ρ/kg·m^{-3}		σ/mN·m^{-1}	
		This paper	Literature	This paper	Literature
283.15	*n*-Butanol	818.90	817.0[16]	25.40	25.4[18], 25.55[19]
293.15	*n*-Butanol	806.20	807.33[17]	24.60	24.60[18], 24.60[18]

Table 5. Densities, surface tensions, and excess surface tensions for the binary systems of x biodiesel+(1−x) *n*-butanol, x biodiesel+(1−x) diesel, x diesel+(1−x) *n*-butanol at temperatures T=(283.15, 293.15) K and atmospheric pressure

x	ρ	ρ^E	ρ	ρ^E	σ	σ^E	σ	σ^E
	kg·m^{-3}				mN·m^{-1}			
	283.15 K		293.15 K		283.15 K		293.15 K	
				x Biodiesel+(1−x) *n*-butanol				
1.0000	891.7	0.00	880.5	0.00	21.10	0.00	19.78	0.00
0.9000	880.7	−3.72	868.8	−4.27	21.19	−0.34	19.84	−0.43
0.7988	871.6	−5.45	859.2	−6.35	21.50	−0.47	20.05	−0.70
0.6999	862.8	−7.05	849.9	−8.30	21.91	−0.48	20.51	−0.72
0.6000	853.9	−8.68	840.5	−10.28	22.39	−0.43	21.07	−0.65
0.4951	847.2	−7.74	833.8	−9.19	22.91	−0.36	21.68	−0.54
0.4001	840.5	−7.53	827.1	−8.83	23.39	−0.29	22.24	−0.44
0.3108	835.6	−5.93	822.3	−6.99	23.83	−0.23	22.76	−0.35
0.1996	828.8	−4.63	815.6	−5.43	24.37	−0.17	23.39	−0.25
0.0999	824.0	−2.17	811.1	−2.52	24.87	−0.10	23.97	−0.14
0.0000	818.9	0.00	806.2	0.00	25.40	0.00	24.60	0.00
				x Biodiesel+(1−x) diesel				
1.0000	891.7	0.00	880.5	0.00	21.10	0.00	19.78	0.00
0.9000	886.0	−0.89	874.2	−1.40	21.78	−0.20	20.45	−0.28
0.8009	880.5	−1.62	868.3	−2.44	22.33	−0.51	20.96	−0.72
0.6998	875.2	−2.06	862.6	−3.19	23.00	−0.73	21.61	−1.03
0.6000	869.9	−2.56	857	−3.90	23.77	−0.84	22.41	−1.18
0.5028	865.5	−2.28	852.7	−3.44	24.67	−0.78	23.40	−1.11
0.4009	860.7	−2.18	847.8	−3.34	25.68	−0.67	24.53	−0.95
0.3005	856.3	−1.75	843.6	−2.62	26.66	−0.57	25.63	−0.80
0.1989	851.8	−1.37	839.2	−2.05	27.73	−0.39	26.85	−0.55
0.1006	847.8	−0.64	835.5	−0.93	28.84	−0.14	28.13	−0.20
0.0000	843.6	0.00	831.5	0.00	29.86	0.00	29.29	0.00
				x Diesel+(1−x) *n*-butanol				
1	843.6	0.00	831.5	0.00	29.86	0.00	29.29	0.00
0.9009	839.4	−1.75	826.6	−2.39	28.46	−0.96	27.69	−1.13
0.8026	836.2	−2.52	822.9	−3.61	27.66	−1.32	26.80	−1.56
0.7044	833	−3.30	819.3	−4.72	27.19	−1.35	26.30	−1.59
0.603	829.7	−4.09	815.7	−5.76	26.88	−1.21	26.00	−1.42
0.5005	827.6	−3.66	813.7	−5.16	26.63	−1.01	25.75	−1.19
0.4009	825.3	−3.50	811.4	−4.94	26.37	−0.82	25.50	−0.96
0.3016	823.6	−2.75	809.9	−3.93	26.10	−0.65	25.24	−0.76
0.2003	821.7	−2.15	808.2	−3.07	25.82	−0.47	24.96	−0.56
0.0995	820.3	−1.06	807.3	−1.42	25.57	−0.27	24.73	−0.32
0	818.9	0.00	806.2	0.00	25.40	0.00	24.58	0.00

(1−x) *n*-butanol, x biodiesel+(1−x) diesel, and x diesel+(1−x) *n*-butanol, and σ^E become more negative when temperature is increased. Tsierkezos and Filippous [24] suggest that the excess surface tensions indicate an uneven distribution of the components between the surface region and the bulk region. They maintain that the negative value of σ^E indicates that the smaller surface tension components have a higher concentration at the liquid surface than its bulk concentration in these binary mixtures. According to this, the smaller surface tension components have a higher concentration at the liquid surface than its bulk concentration. To our knowledge, the values of σ^E from our results for diesel+n-butanol have similar trends compared with the literature values [8]. For excess densities, as shown in Table 5 and Fig. 4, the ρ^E values were all negative, and display the minimum at x≈0.6, 0.6, 0.6 for x biodiesel+(1−x) *n*-butanol, x biodiesel+(1−x) diesel, and x diesel+(1−x) *n*-butanol, respectively. For biodiesel+diesel, the ρ^E values were all negative and decreased with the increasing the temperature, which can be attributed to the strong interactions between the similar molecules. To our knowledge, the ρ^E values were consistent with the conclusion of Mesquita et al. [25] under room temperature. While for diesel+n-butanol and diesel+*n*-butanol mixtures, the negative ρ^E values may result from the weak interaction between

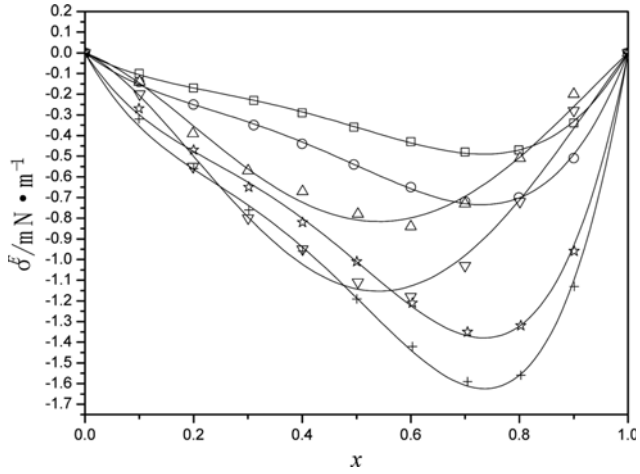

Fig. 3. Excess surface tension σ^E against mass fraction x of binary mixture: x biodiesel+(1−x) *n*-butanol, □ 283.15 K, ○ 298.15 K; x biodiesel+(1−x) diesel, △ 283.15 K, ▽ 293.15 K; and x diesel+(1−x) *n*-butanol, ☆ 283.15 K, + 293.15 K. Solid lines show results calculated using the Redlich-Kister equation.

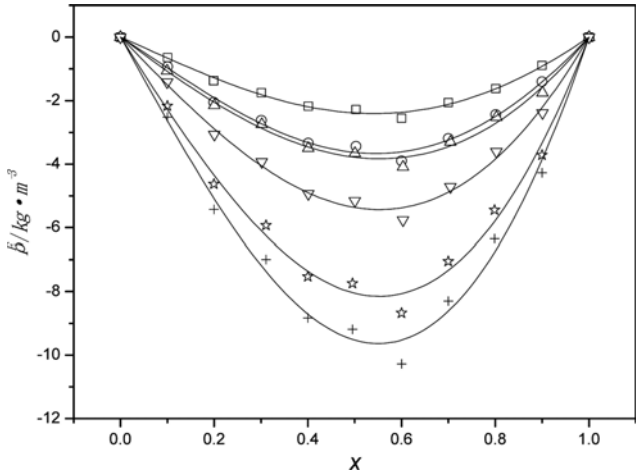

Fig. 4. Excess densities ρ^E against mass fraction *x* of binary mixture: x biodiesel+(1−x) *n*-butanol, □ 283.15 K, ○ 293.15 K; x biodiesel+(1−x) diesel, △ 283.15 K, ▽ 293.15 K; and x diesel+(1−x) *n*-butanol, ☆ 283.15 K, + 293.15 K. Solid lines show results calculated using the Redlich-Kister equation.

Table 6. Fitting parameters and standard errors

	T/K	A_0	A_1	A_2	Standard errors
		σ^E/mN·m^{-1}			
x Biodiesel+(1−x) *n*-butanol	283.15	−1.4400	−1.5616	−1.5471	0.0051
	293.15	−2.1793	−2.3500	−2.2039	0.0232
x Biodiesel+(1−x) diesel	283.15	−3.2300	−0.7899	1.5110	0.0387
	293.15	−4.5666	−1.1066	2.1678	0.0526
x Diesel+(1−x) *n*-butanol	283.15	−4.0385	−4.4057	−4.3956	0.0205
	293.15	−4.7401	−5.1926	−5.2559	0.0229
		ρ^E/kg·m^{-3}			
x Biodiesel+(1−x) *n*-butanol	283.15	−32.1999	−7.3588	1.5117	0.0731
	293.15	−38.1126	−8.5460	3.2210	0.0712
x Biodiesel+(1−x) diesel	283.15	−9.5478	−1.8217	1.2399	0.0352
	293.15	−14.5305	−3.0821	2.0620	0.0646
x Diesel+(1−x) *n*-butanol	283.15	−15.1323	−3.5005	0.6029	0.0629
	293.15	−21.4613	−4.9847	1.1753	0.0796

different molecules.

CONCLUSION

Densities and surface tensions were measured at 283.15 K and 293.15 K for biodiesel+*n*-butanol, biodiesel+diesel, diesel+*n*-butanol binary mixtures. For densities and surface tensions, the combined expanded uncertainty was 1.32 kg·m^{-3} and 1%, respectively. The excess surface tensions and densities were negative over the entire composition range at all temperatures, and further fitted to the Redlich-Kister equation.

ACKNOWLEDGEMENTS

The authors acknowledge the financial support of the National Natural Science Foundation of China (No. 51376149).

REFERENCES

1. F. Lujaji, A. Bereczky and M. Mbarawa, *Energy Fuels*, **24**, 4490 (2010).
2. Z. Huang, H. Miao, L. Zhou and D. Jiang, *P. I. Mech. Eng. D-J. Aut.*, **214**, 341 (2000).
3. M. Noboru, O. Hideyuki and O. Kohichi, *JASE Review*, **19**, 154 (1988).
4. L. Zhu, C. S. Cheung, W. G. Zhang and Z. Huang, *Sci. Total Environ.*, **408**, 914 (2010).
5. Z. Bo, F. Weibiao and G. Jingsong, *Fuel*, **85**, 778 (2006).
6. E. Alptekin and M. Canakci, *Renewable Energy*, **33**, 2623 (2008).
7. N. P. Bahadur, D. G. B. Boocock and S. K. Konar, *Energy Fuels*, **9**, 248 (1995).
8. P. Deng, R. Huang, Y. Ma and H. Dai, *SAE Technical. Paper.*, 2013-01-2598 (2013).

9. F. K. Wang, J. T. Wu and Z. G. Liu, *Energy Fuels*, **20**, 2471 (2006).
10. T. Nishio and Y. Nagasaka, *Int. J. Thermophysics*, **16**, 1087 (1995).
11. K. U. Ingrad, Fundamentals of Waves & Oscillations, Great Britain: the University Press, Cambridge, 478 (1988).
12. K. U. Ingard, Fundamentals of Waves & Oscillations, U.K. (1988).
13. Y. Y. An, J. F. Liu and Q. H. Li, Optoelectronic Technology, Beijing (2002).
14. ISO, Guide to the Expression of Uncertainty in Measurement. *International Organisation for Standardisation, Switzerland*. 9-71 (1995).
15. G. J. Zhao, Development of Surface Laser Light Scattering Apparatus for Liquid Viscosity and Surface Tension Measurement and Its Applications, Xi'an, Xi'an Jiao Tong University (2006).
16. C. Valles, E. Perez, M. Cardoso, M. Dominguez and A. M. Mainar, *J. Chem. Eng. Data*, **49**, 1460 (2004).
17. T. Reza, M. Hamid and S. John, *J. Chem. Eng. Data*, **51**, 1039 (2006).
18. C. Wohlfarth and B. Wohlfarth, Surface Tension of Pure Liquids and Binary Liquid Mixtures, Volume 16, Springer-Verlag (1997).
19. B. Giner, A. Villares, S. Martin, H. Artigas and C. Lafuente, *J. Chem. Eng. Data*, **52**, 1904 (2007).
20. C. R. Pan, Q. F. Ke, G. F. Ouyang, X. H. Zhen, Y. Y. Yang and Z. Q. Huang, *J. Chem. Eng. Data*, **49**, 1839 (2004).
21. J. Vijande, M. M. Pineiro, J. Garcia, J. L. Valencia and J. L. Legido, *J. Chem. Eng. Data*, **51**, 1778 (2006).
22. O. Redlich and A. Kister, *Ind. Eng. Chem.*, **40**, 345 (1948).
23. A. A. Mohammad, A. K. H. E. Mohammad, M. S. Altuwaim and A. S. Al-Jimaz, *J. Chem. Thermodynamics*, **56**, 106 (2013).
24. N. G. Tsierkezos and A. C. Filippous, *J. Chem. Thermodynamics*, **38**, 952 (2006).
25. F. M. R. Mesquita, F. X. Feitosa, R. S. Santiago and H. B. de Sant'Ana, *J. Chem. Eng. Data*, **56**, 153 (2011).